

# Gas-Phase Electron Diffraction Study of Hexakis-(dimethylamido)tungsten(VI), $W(NMe_2)_6$

Kolbjørn Hagen,<sup>a</sup> Catherine J. Holwill,<sup>b</sup> David A. Rice<sup>b</sup> and Jonathan D. Runnacles<sup>c</sup>

<sup>a</sup>The Department of Chemistry, The University of Trondheim, N-7055 Dragvoll, Trondheim, Norway, <sup>b</sup>The Department of Chemistry, The University of Reading, Whiteknights, Reading RG6 2AD and <sup>c</sup>The Department of Chemistry, Queen Mary College, Mile End Road, London, U.K.

Hagen, K., Holwill, C. J., Rice, D. A. and Runnacles, J. D., 1988. Gas-Phase Electron Diffraction Study of Hexakis(dimethylamido)tungsten(VI),  $W(NMe_2)_6$ . – Acta Chem. Scand., Ser. A 42: 578–583.

The molecular structure of  $W(NMe_2)_6$  has been studied by gas-phase electron diffraction. The experimental data are fitted by a model that contains three orthogonal planar  $C_2N-W-NC_2$  units (with  $\angle N-W-N = 180^\circ$ ); thus, the  $W(NC_2)_6$  core has  $T_h$  symmetry. The values, with estimates of uncertainties ( $2\sigma$ ), for the principal distances ( $r_g$ ) and angles ( $\angle_g$ ) are:  $r_g(W-N) = 2.035(5)$  Å,  $r_g(C-N) = 1.453(4)$  Å,  $r_g(C-H) = 1.064(7)$  Å,  $\angle W-N-C = 125.6(4)^\circ$ , and  $\angle N-C-H = 113.6(21)^\circ$ .

**Dedicated to Professor Otto Bastiansen on his 70th birthday**

Few octahedral binary, or pseudo-binary, compounds of tungsten(VI) are known. For example, of the halides only fluorine and chlorine form stable hexahalides. Although it is claimed the bromide,  $WBr_6$ , can be obtained by allowing  $W(CO)_6$  to react with an excess of bromine, the exact nature of the product has not been ascertained and it certainly evolves bromine when warmed to above room temperature. It is therefore surprising that reaction of tungsten(VI) chloride with either  $LiMe$  or  $LiNMe_2$  gives the species  $WMe_6$ <sup>1</sup> and  $W(NMe_2)_6$ ,<sup>2</sup> respectively together with some lower oxidation state tungsten compounds. The compound  $W(NMe_2)_6$  has been the subject of a single crystal X-ray study and shown to consist of isolated  $W(NMe_2)_6$  molecules containing octahedral  $WN_6$  moieties. Unfortunately the X-ray study revealed that the crystals exhibited some disorder. However, it is known that the compound has a considerable vapour pressure at 220 °C and is likely to form molecules with high symmetry in the gas phase. Thus, molecular  $W(NMe_2)_6$  is suitable for a structural investigation by gas-phase electron diffraction. Accordingly we have carried out a gas-phase electron diffraction study of  $W(NMe_2)_6$ , and we compare

the results with those provided by the X-ray investigation.<sup>2</sup> Also available for comparison are data from an electron diffraction study of  $Zr(NMe_2)_6$ ,<sup>3</sup> which has been shown to contain a  $T_d$   $ZrN_4$  core and planar  $Zr-N-C_2$  fragments; thus, the  $Zr(N-C_2)_4$  framework had  $D_{2d}$  symmetry.

## Experimental and analysis of the structure

*Preparation of  $W(NMe_2)_6$ .* Using "Schlenk" tube procedures,  $W(NMe_2)_6$  was prepared by allowing  $WCl_6$  to react with  $LiNMe_2$  according to published procedures.<sup>2</sup> The product was purified by sublimation and samples (approximately 1 g) were placed in sealed ampoules which could be loaded directly into the Balzers Eldigraph KDG-2 apparatus at the University of Oslo<sup>4,5</sup> and opened *in situ*.

Data were obtained at nozzle-to-plate distances of 497.95 mm and 248.12 mm with nozzle temperatures of 220–230 °C. The electron wavelength was calibrated against diffraction pictures for benzene.<sup>6</sup> Five plates for both camera distances were used in the final analysis. The data

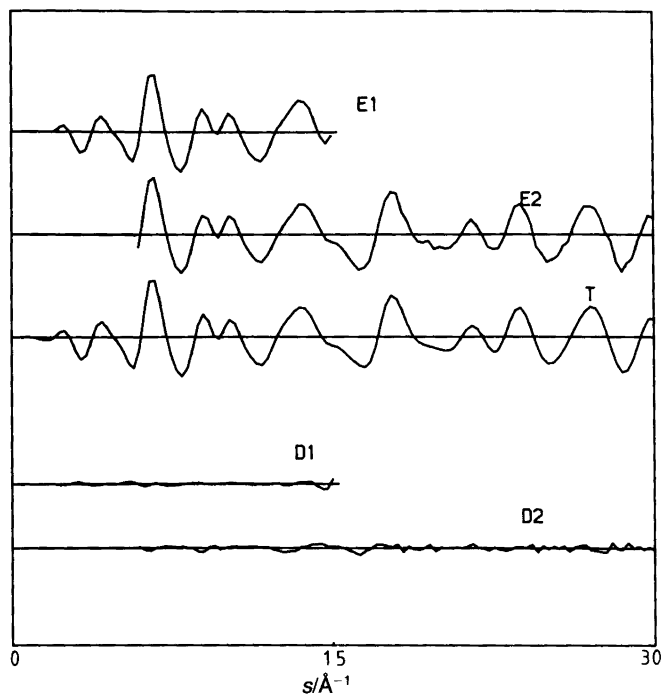


Fig. 1. Intensity curves  $sI_m(s)$  for  $W(NMe_2)_6$ . Experimental curves (E1 and E2) are averages for all plates for the two camera distances. The theoretical curve (T) was calculated from the structural parameters shown in Table 1 using mercury phase-shift factors. The difference curves (D1 and D2) result from the subtraction of the relevant part of the theoretical curve from the experimental curves.

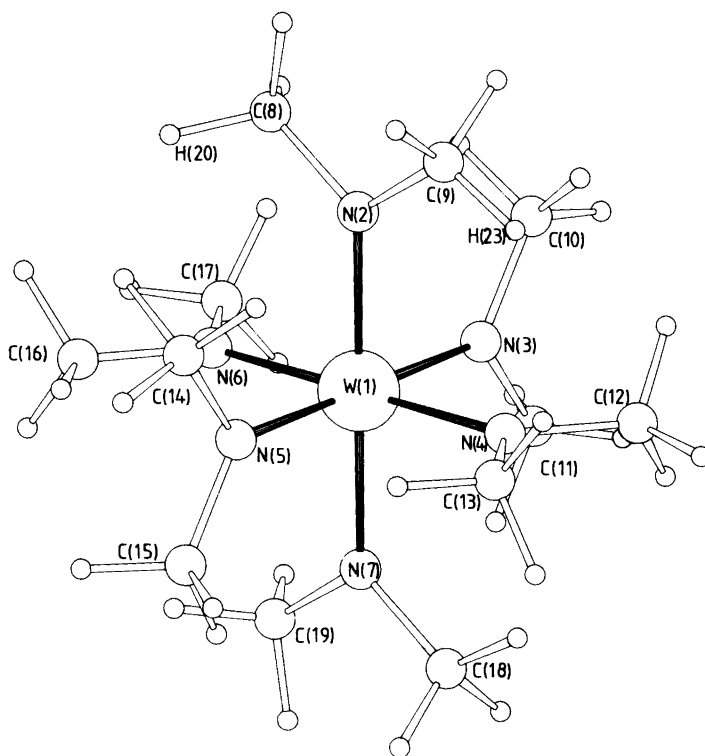


Fig. 2. The atom numbering scheme used in the study of  $W(NMe_2)_6$ . The hydrogen atoms are numbered in sequence starting with those bound to the carbon atom with the lowest number. Thus,  $H_{20}$ ,  $H_{21}$  and  $H_{22}$  are bound to C8. The two hydrogen atoms ( $H_{20}$  and  $H_{23}$ ) atoms that take part in the torsion angles  $\varphi_1$  and  $\varphi_2$  are specified in the figure.

cover the ranges  $2.00 < s < 15.00 \text{ \AA}^{-1}$  and  $4.00 < s < 30.00 \text{ \AA}^{-1}$  at intervals of  $s = 0.25 \text{ \AA}^{-1}$ . The experimental data were processed as previously described,<sup>7-11</sup> with scattering factors taken from Refs. 12 and 13. Refinements of the structure were carried out by the least-squares method<sup>14</sup> by adjusting one theoretical curve to fit the two average experimental intensity curves (one for each of the two nozzle-to-plate distances) using a unit weight matrix. The average curves, the final theoretical curve and the difference curves are depicted in Fig. 1. The reduced intensity data and the background curves are available as supplementary data.

Fig. 2 shows a representation of the molecule together with the atom numbering scheme that was used for the tungsten, nitrogen and carbon atoms. Only a few hydrogen atoms are numbered; they are numbered in sequence, with those having the lowest numbers being bonded to C(8) and those with the highest numbers are bonded

to C(19). It was assumed that the  $\text{WN}_6$  moiety has  $O_h$  symmetry and that the  $\text{C}_2\text{NWC}_2$  fragments are planar. In early refinements the  $\text{C}_2\text{NWC}_2$  fragments were allowed to deviate from planarity. The deviations were found to be small ( $2.0$  to  $3.0^\circ$ ) and the standard deviation associated with the angle was large enough to make the deviation not significant. Thus, the model adopted for the refinement can be described in terms of three bonded distances, viz.  $r(\text{W}-\text{N})$ ,  $r(\text{N}-\text{C})$  and  $r(\text{C}-\text{H})$ , two valence angles, viz.  $\angle\text{N}-\text{C}-\text{H}$  and  $\angle\text{W}-\text{N}-\text{C}$ , and two torsion angles  $\varphi_1$  (which is  $\angle\text{H}_{20}-\text{C}_8-\text{N}_2-\text{W}$ ) and  $\varphi_2$  (which is  $\angle\text{H}_{23}-\text{C}_9-\text{N}_2-\text{W}$ ). The two torsion angles were defined to allow the two methyl groups to rotate independently of each other about their  $\text{N}-\text{C}$  bonds. However, refinement of these two torsion angles gave values that carried a high degree of uncertainty. Accordingly, refinements were carried out in which  $\varphi_1$  was allowed to refine while  $\varphi_2$  was varied at  $2^\circ$

Table 1. Final structural parameters for  $\text{W}(\text{NMe}_2)_6$ .<sup>a</sup>

Parameter	$r_g/\angle\alpha$		$l_{\text{refined}}$		$l_{\text{calc}}$
	W <sup>b</sup>	Hg <sup>c</sup>	W <sup>b</sup>	Hg <sup>c</sup>	
Independent parameters					
$r_g(\text{W}-\text{N})$	2.034(5)	2.035(5)	0.058(2)	0.061(2)	0.060
$r_g(\text{C}_8-\text{N}_2)$	1.452(5)	1.453(4)	0.046(5)	0.047(4)	0.054
$r_g(\text{C}-\text{H})$	1.068(9)	1.064(7)	0.078(11)	0.079(10)	0.069
$\angle\text{W}-\text{N}_2-\text{C}_8$	125.9(5)	125.6(4)			
$\angle\text{N}_2-\text{C}_8-\text{H}_{20}$	112.6(22)	113.6(21)			
$\varphi_1^d$		55.6	55.6		
$\varphi_2^d$		38.4	38.4		
Selected Dependent parameters					
$r_g(\text{C}_8\cdots\text{C}_9)$	2.380(16)	2.379(15)	0.085(4)	0.088(2)	0.095
$r_g(\text{N}_2\cdots\text{N}_3)$	2.877(7)	2.883(7)	0.082(14)	0.107(11)	0.080
$r_g(\text{C}_{10}\cdots\text{N}_2)$	3.016(6)	3.011(7)	0.109(14)	0.115(11)	0.121
$r_g(\text{N}_2\cdots\text{N}_7)$	4.068(9)	4.073(9)	0.081(11)	0.077(10)	0.081
$r_g(\text{W}\cdots\text{C}_8)$	3.126(7)	3.126(7)	0.084(8)	0.085(8)	0.084
$\angle\text{C}_8-\text{N}_2-\text{C}_9$	108.2(10)	108.9(8)			
<i>R</i> factors					
Long camera dist.	0.086	0.086			
Short camera dist.	0.119	0.096			

<sup>a</sup>Distances in  $\text{\AA}$  and angles in degrees. Errors are  $2\sigma$ , including an estimate of errors in wavelength etc.,

<sup>b</sup>Refinement in which the phase-shift factors for tungsten were used. <sup>c</sup>Refinement in which the phase-shift factors for tungsten were replaced with those of mercury. <sup>d</sup> $\varphi_1$  is the torsion angle  $\angle\text{H}_{20}-\text{C}_8-\text{N}_2-\text{W}$ , while  $\varphi_2$  is the torsion angle  $\angle\text{H}_{23}-\text{C}_9-\text{N}_2-\text{W}$ .

intervals from  $0^\circ$  to  $60^\circ$ . Having determined the best value for  $\varphi_1$  it was fixed, and  $\varphi_2$  was allowed to refine from its value which gave the best value for  $\varphi_2$ . The resulting values are given in Table 1. The methyl groups were assumed to have  $C_{3v}$  symmetry, with the three-fold axis coinciding with the C–N bond.

Root-mean-square vibrational amplitudes ( $l$ ) were calculated from an assumed valence force field using values for the force constants obtained from studies of related molecules.

In the final refinement all the independent variables (except  $\varphi_1$  and  $\varphi_2$ ) were allowed to refine together with the vibrational amplitudes associated with the bonded distances. Those vibrational amplitudes associated with the non-bonded interactions that were thought to be most influential on the structure [ $l(C_8 \cdots C_9)$ ,  $l(C_{10} \cdots N_2)$ ,  $l(W \cdots C_8)$ ,  $l(N_2 \cdots N_3)$  and  $l(N_2 \cdots N_7)$ ] were allowed to refine; the remaining amplitudes were kept constant at the calculated values. The radial distribution (RD) curves were calculated in the usual manner by Fourier transformation of the  $s[I_m(s)]$  values after multiplication by  $(Z_W Z_N / f_W f_N) \exp(-0.0025 s^2)$ .

In our study of  $OsOCl_4$ <sup>10</sup> we found that an

improved fit to the experimental data was obtained when the osmium phase-shift factors were replaced by those for lead. Accordingly, an investigation into the effect of substituting the phase-shift factors for tungsten was carried out and it was found that the best fit was obtained using the data for mercury. Changing the phase-shift factors from those for tungsten to those for mercury has no effect on the geometry, although lower standard deviations and  $R$  factors are obtained with the latter (see Table 1). In the radial distribution curve there is an improvement in fit around  $2.04 \text{ \AA}$ . Besides errors in the phase-shift factors, the failure to take into account three-atom scattering may be a cause of the difference between the theoretical and experimental radial distribution curves. However, although we had previously attempted to allow for three-atom scattering, there was no improvement in the fit between theory and experiment. In Fig. 3 are depicted the experimental, theoretical and difference radial distribution curves calculated using the curves derived with the phase-shift factors for mercury. The results of the final refinement are shown in Table 1, while Table 2 contains the correlation matrix for the refined parameters.

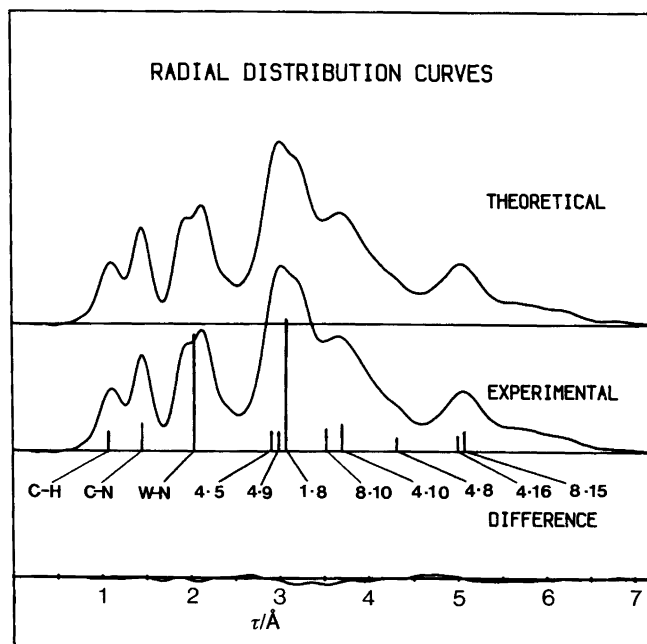


Fig. 3. Radial distribution curves for  $W(NMe_2)_6$ , showing the experimental, theoretical and difference curves. The curves were calculated from the curve in Fig. 1 after multiplication by  $Z_W Z_N / f_W f_N \exp(-0.0025 s^2)$  and using theoretical data for the unobserved region  $s < 2.0 \text{ \AA}^{-1}$ . The vertical lines indicate the locations and weights of some of the more important distances in the molecule, the atomic numbering being given in Fig. 2.

Table 2. Correlation matrix ( $\times 100$ ) for the parameters in  $W(NMe_2)_6$ .

Parameter	$\sigma LS^a$	$r_1$	$r_2$	$r_3$	$\angle_4$	$\angle_5$	$l_6$	$l_7$	$l_8$	$l_9$	$l_{10}$	$l_{11}$	$l_{12}$	$l_{13}$
1. $r(W-N)$	0.0009	100	-20	1	-40	-15	6	6	5	27	-34	8	16	0
2. $r(C_8-N_2)$	0.0010		100	12	-19	10	10	3	12	3	5	5	4	1
3. $r(C-H)$	0.0027			100	-8	-10	-1	3	6	9	-3	5	8	1
4. $\angle W-N_2-C_8$	0.15				100	-22	-10	-12	-18	-48	22	-26	-65	-6
5. $\angle N_2-C_8-H_{20}$	0.76					100	5	10	10	16	9	12	23	6
6. $l(C-H)$	0.0025						100	28	18	15	-8	9	10	-2
7. $l(C_8-N_2)$	0.0013							100	17	24	-12	20	21	-1
8. $l(W-N)$	0.0007								100	26	-16	15	23	-1
9. $l(C_{10}\cdots N_2)$	0.0079									100	-17	11	47	4
10. $l(C_8\cdots C_8)$	0.0067										100	-13	-23	-2
11. $l(W\cdots C_8)$	0.0013											100	49	3
12. $l(N_2\cdots N_3)$	0.0047												100	7
13. $l(N_2\cdots N_7)$	0.0158													100

<sup>a</sup>Standard deviations taken from the least-squares refinement. Distances ( $r$ ) and amplitude ( $l$ ) in Å, angles in degrees.

## Results and discussion

The results obtained in our study of  $W(NMe_2)_6$  are consistent with the molecule having  $T_h$  symmetry in the gas phase, which is similar to the situation observed in the solid state.<sup>2</sup> The metal–nitrogen distance [ $r_g(W-N) = 2.035(5)$  Å] is in agreement with that observed in the solid state [ $2.032(25)$  Å]<sup>2</sup> but shorter than that found in  $Zr(NMe_2)_4$  [ $r_g(Zr-N) = 2.071(11)$  Å].<sup>3</sup> However, the difference is less than the difference between the covalent radii of zirconium and tungsten (0.15 Å), which is an observation that can be understood by considering the different roles of the lone-pair electrons in the two molecules. Of the twenty-four electrons available for bonding in the  $WN_6$  fragment, twelve are used in  $\sigma$  bonding. The remaining twelve are in six lone pairs (one on each nitrogen atom), and in the  $T_h$  point group these lone pairs transform as  $T_{2g}$  and  $T_{1u}$ . The  $T_{2g}$  set is able to combine with the  $T_{2g}$  set of tungsten metal orbitals ( $5d_{xy}$ ,  $5d_{xz}$  and  $5d_{yz}$ ), while the  $T_{1u}$  set is essentially non-bonding as the only metal atomic orbitals with  $T_{1u}$  symmetry ( $6p_x$ ,  $6p_y$ ,  $6p_z$ ) are used for  $\sigma$  bonding. Thus, the tungsten–nitrogen bonds can be visualised as being of order 1.5. In contrast there are sixteen electrons available for bonding in the  $ZrN_4$  fragment of  $D_{2d}$  symmetry found in  $Zr(NMe_2)_4$ .<sup>3</sup> Both the four  $Zr-N$  sigma bonds and the four lone pairs on the nitrogen atoms transform as  $A_1$ ,  $B_2$  and  $E$ . For

the  $\sigma$  bonds the following metal orbitals are available:  $5s$  ( $A_1$ ),  $5p_z$  ( $B_2$ ) and  $5p_x$  with  $5p_y$  ( $E$ ), while the  $\pi$  bonding can be accommodated by  $4d_{z^2}$  ( $A_1$ ),  $4d_{xy}$  ( $B_1$ ), and  $4d_{yz}$  with  $4d_{xz}$  ( $E$ ). Thus, in contrast to the  $W-N$  bonds in  $W(NMe_2)_6$ , the  $Zr-N$  bonds in  $Zr(NMe_2)_4$  can be envisaged as double bonds; it is therefore to be expected that the difference between  $r_g(Zr-N)$  and  $r_g(W-N)$  will be less than the difference between the covalent radii of the two metals. The zirconium compound presents an unusual situation. Rotation of the  $N-C_2$  groups in a concerted manner about the  $Zr-N$  bond does not destroy the double-bond character; even if the symmetry of the molecule decreased to be  $S_4$ , the multiple-bond character would be maintained. Thus, any difference in rigidity between  $Zr(NMe_2)_4$  and  $W(NMe_2)_6$  must be an effect of the difference in metal covalent radii and coordination number between  $W(NMe_2)_6$  and  $Zr(NMe_2)_4$ . This is illustrated by the difference in the  $l(M\cdots C)$  values [for  $M = W$  it is  $0.085(1)$  Å; for  $M = Zr$  it is  $0.160(9)$  Å], while the  $l(C\cdots C)$  values are equivalent. Furthermore, the barrier to rotation about the  $M-N$  bonds is greater in the tungsten compound than in the zirconium species, as shown by the high degree of uncertainty found for the  $C-N_1-Zr-N_2$  angle [ $109.7(87)^\circ$ ] and the planarity found in the present study for the  $C_2N-W-NC_2$  fragments in  $W(NMe_2)_6$ . At  $125.6$  ( $4$ ) $^\circ$  the  $W-N-C$  angle is smaller than that seen

in the solid state<sup>2</sup> (127.5°) but in accord with that seen in  $Zr(NMe_2)_4^3$  [124.3(6)°]. The  $r_g(C-N)$  [1.453(4) Å] is shorter than observed in the solid state (1.516 Å) but in agreement with the values found in the gas phase for  $Sn(NMe_2)_4^{15}$  [1.450(19) Å] and  $Zr(NMe_2)_4^3$  [1.461(4) Å].

**Acknowledgements.** We gratefully acknowledge the help and interest of Professor Otto Bastiansen, and wish to thank him for making electron diffraction facilities available to C.J.H. and D.A.R., enabling them to gain the necessary experience to establish an electron diffraction apparatus in Reading.

We thank Professor D. C. Bradley of Queen Mary College, London, for his interest in the work, and Snefrid Gundersen and Hans Volden of the University of Oslo for their technical help. We also thank the S.E.R.C. for financial support to C.J.H. and J.D.R., and NATO for the award of a travel grant (No. 117/82).

## References

1. (a) Mertis, K. and Wilkinson, G. *J. Chem. Soc., Dalton Trans.* (1976) 1488; (b) Galyer, A. and Wilkinson, G. *J. Chem. Soc., Dalton Trans.* (1976) 2235.
2. Bradley, D. C., Chisholm, M. H., Heath, C. E. and Hursthouse, M. B. *J. Chem. Soc., Chem. Commun.* (1969) 1261.
3. Hagen, K., Holwill, C. J., Rice, D. A. and Runnacles, J. D. *Inorg. Chem.* 27 (1988) 2032.
4. Zeil, W., Haase, J. and Wegmann, L. *Z. Instrumentenk. 74* (1966) 84.
5. Bastiansen, O., Graber, G. and Wegmann, L. *Balzers' High Vacuum Report 25* (1969) 1.
6. Tamagawa, K., Iijima, T. and Kimura, M. *J. Mol. Struct.* 30 (1976) 243.
7. Hagen, K. and Hedberg, K. *J. Am. Chem. Soc.* 95 (1973) 1003.
8. Gundersen, G. and Hedberg, K. *J. Chem. Phys.* 51 (1969) 2500.
9. Andersen, B., Seip, H. M., Strand, T. G. and Stølevik, R. *Acta Chem. Scand.* 23 (1969) 3224.
10. Hagen, K., Hobson, R. J., Holwill, C. J. and Rice, D. A. *Inorg. Chem.* 25 (1986) 3659.
11. Hedberg, L. *Abstracts of 5th Austin Symposium on Gas-Phase Molecular Structure*, Austin, TX, Mar. 1974, p. 37.
12. *International Tables for X-Ray Crystallography*, Kynoch Press, Birmingham 1974.
13. Sellers, H. L., Schafer, L. and Bonham, R. A. *J. Mol. Struct.* 49 (1978) 125.
14. Hedberg, K. and Iwasaki, M. *Acta Crystallogr.* 17 (1964) 529.
15. Vilkov, L. V., Tarasenko, N. A. and Prokofev, A. K. *Zh. Strukt. Khim.* 11 (1970) 129.

Received January 29, 1988.